Indian J. Phys. 76B (4), 393–400 (2002)

IJP B
— an international journal

Inner shell ionisation with low velocity heavy ions

Manoranjan Sarkar
Saha Institute of Nuclear Physics, 1/AF, Bidhannagar, Kolkata-700 064, India
E-mail : mano@anp.saha.ernet.in

Abstract : Inner shell ionisation with protons and alphas has been studied extensively for the last few decades but data with heavy ions are really scarce. With proton or helium, the coulombic interaction between the projectile and the electron can be well treated with the existing theories but with the low velocity heavy ions with their electron clouds, the perturbation becomes stronger and the normal collision dynamics gets modified. In order to investigate this effect, we used C and O ions from the 3 MeV Pelletron at IOP Bhubaneswar in the energy range of 4–12 MeV to measure the *K*, *L* and *M* cross sections of different elements like Ge, Ag, Au, Pb and Bi. We have also measured the anisotropy and the alignment parameters of the induced ions and the results were then compared with ECPSSR theory In the case of *L* subshells, it was observed that the Intra-shell effect plays a significant rule at such low velocities.

Keywords . Inner shell ionization, low velocity, heavy ions

PACS No. : 34.80.Dp

1. Introduction

After the discovery of X-rays by Röntgen [1], Chadwick [2] first observed the characteristic X-rays from several elements by exposing them to alpha particles emitted from a radium source. In a similar fashion, Franz and Bothe [3] observed *K*, *L* and *M* shell X-rays from elements $Z = 32$–79 and 83. The first successful experiment to produce target X-rays by bombarding with proton was done by Grethsen and Reusse 4]. Peter [5] and Livingston *et al* [6] also studied characteristic X-rays produced by bombarding with protons upto the energy of 1.76 MeV.

All these early works are the basis of our present day activities on Inner Shell Ionisation (ISI) in ion-atom collision. With the availability of large number of particle accelerators, advancement in detection systems, data acquisition and analysis, activities on ISI have got a tremendous boost during the last few decades. The reasons behind the activities in ISI were two fold. (i) Proton induced *K* and *L* shell X-ray production cross sections of different elements were of urgent need as inputs to the one of the most powerful micro- analytical technique called PIXE which was started in the seventies by a group from Lund University [7] and (ii) to understand the mechanism of ISI in the light of the existing theories on ion-atom collision.

To understand the mechanism of inner-shell ionisation in ion-atom collision, several theories such as Plane Wave Born Approximation (PWBA) [8–11], Binary Encounter Approximation (BEA) [12] and Semi-Classical Approximation (SCA) [13,14] have been formulated. Corrections due to the projectile energy loss (*E*), coulomb deflection of the projectile in the field of the target nucleus (*C*), relativistic nature of the inner-shell electrons (*R*) and the polarisation and increased binding of the inner-shell electrons have been introduced into the PWBA formalism through Perturbed Stationary State (PSS) [15] calculation, which is known and abbreviated as ECPSSR. In PIXE work, the ECPSSR theory has received wide acceptance and comparison of this theory with the experimental data on *K* shell ionisation are also within a few percent [16].

The reasons for our investigation of ISI with low velocity heavy ions are : (i) at low velocity compared to the velocity of the orbital electron some strange and peculiar phenomena occur especially with heavy ions which are difficult to explain with the existing theories and (ii) most of the ISI

measurements done previously were with protons or alpha particles, where existing theoretical predictions are quite good. But the measurements with heavy ions are still scarce. And so the existing theoretical models could be best tested with the data of heavy ions where the collision mechanism is more complicated than with single particles like protons.

In this talk, I would like to present before you some of our activities on ISI that we have been carrying out for the last 5–6 years with low velocity heavy ions obtained from the Pelletron Accelerator of the Institute of Physics, Bhubaneswar. First of all, I shall describe briefly about our experimental set up and then pass on to *L*, *M* and *K* shell measurements.

2. Experimental

All the measurements were done using the 3MV 9SDH-2 Tandem Pelletron at the Institute of Physics, Bhubaneswar. The energy range of the projectiles was 0.25 to 1.1 MeV/amu. Figure 1 shows a schematic diagram of the

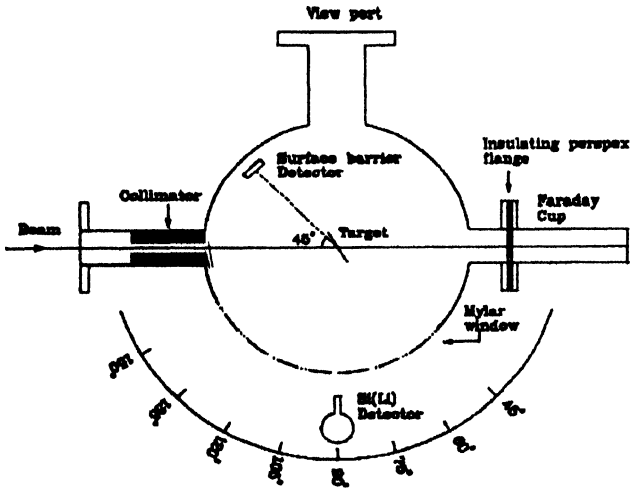

Figure 1. Schematic diagram of the scattering chamber.

vacuum chamber (diameter = 28 cm) used in these measurements. The beam enters the chamber through two carbon slits of diameter 3 mm separated by a distance of 7.5 cm. A Si(Li) detector having a resolution of 160 eV at 5.9 keV was used for the measurements. For the cross section measurement, the detector was placed at an angle of 90° to the beam. Eight holes each with a diameter of ~12 mm were made on the wall of the scattering chamber at angular positions of 150°, 135°, 120°, 105°, 90°, 75°, 60° and 45°. These holes were vacuum sealed with mylar of thickness 3.8 mg/cm^2. For the angular distribution study, the Si(Li) was placed at each of these holes with the help of an angular distribution table. For the normalisation of the beam intensity, a surface barrier detector was placed inside the chamber at an angle of 135°. With our target mounting system, three targets could be placed inside the chamber at a time inside the chamber. The slots in the target mount could automatically bring the target at the center of the chamber. The count rate during each run was kept below 1000/sec so as to avoid any pile up effect. The X-ray pulses were processed through a preamplifier, an amplifier, an ADC and finally fed to an MCA. The targets used in the different measurements are shown in Table 1.

Table 1. Targets used for the cross section and angular distribution measurements.

Element	Target thickness (μg/cm^2)	Backing material
Au	70	*C* (20 μg/cm^2)
Au	75	*C* (10 μg/cm^2)
Au	50	*C* (10 μg/cm^2)
Au	150	self supporting
Bi	200	*C* (10 μg/cm^2)
Ge	70	*C* (10 μg/cm^2)
Ag	70	*C* (10 μg/cm^2)

3.1. L Shell measurement

a. Cross section measurement :

A typical gold *L* spectrum induced by 4.3 MeV carbon ions is shown in Figure 2.

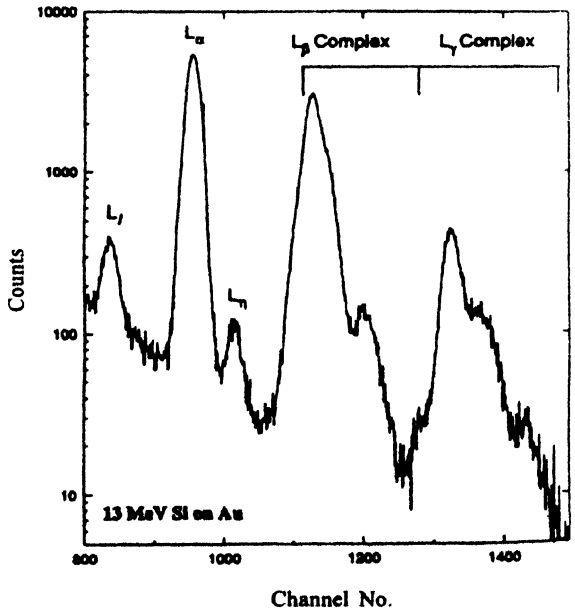

Figure 2. *L* X-ray spectrum of Au induced by 4.3 MeV carbon ions

For the evaluation of X-ray production cross section the following relations were used :

$$N_x = N_0 N_t \sigma^x \varepsilon' F \quad (1)$$

$$N_p = N_0 N_t \sigma^R(\theta)(d\Omega)_p \quad (2)$$

where N_x = X-ray peak intensity

N_0 = Number of incident particles

N_t = Number of target atoms

σ^x = X-ray production cross section

ε' = Effective efficiency of the Si(Li) detector

F = Correction factor due to slowing down of theprojectile and X-ray self absorption inside the target

N_p = Back scattered peak intensity

$\sigma^R(\theta)$ = Rutherford scattering cross section at an angle θ

$(d\Omega)_p$ = Solid angle subtended by the surface barrier detector

sing relations (1) and (2), the X-ray production cross ction can be expressed as

$$\sigma^x = \frac{N_x \sigma^R(\theta)(d\Omega)_p}{N_p \varepsilon' F} \tag{3}$$

ıe efficiency of the Si(Li) detector were measured using librated radioactive sources of Fe^{55} and Am^{241}. Elemental 'gets of Al, Si and P were also excited with 2 MeV protons get the efficiency values at lower energies. Following the ethod of Datz *et al* [17] ionisation cross sections of $L1$, $L2$ d $L3$ subshells of Au and Bi induced by C and O ions ere obtained [18]. As a typical example, Figure 3 shows the perimental values of $L1$, $L2$ and $L3$ subshell ionisation oss section of Au induced by O ions.

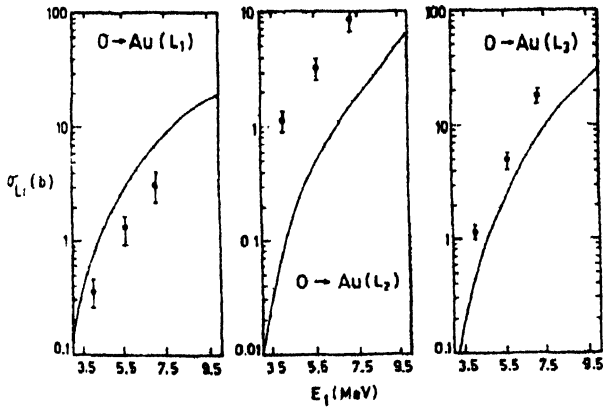

ure 3. $L1$, $L2$ and $L3$ subshell ionisation of Au induced O ions. CPSSR, • present data.

It is observed that the ECPSSR predictions are not very from our experimental values of $L1$ and $L3$, but the oretical prediction for $L2$ is a factor of 10 less than the erimental results. This tendency remains almost the same case of carbon ion bombardment also. This type of crepancy could neither be explained with the help of ltiple outer shell ionisation nor with the uncertainty ociated with the atomic parameters used to convert the ay production cross sections to subshell ionisation cross tions.

Having faced the problem, we tried to find out the main reason behind the mismatch. Sarkadi and Mukoyama [19] had first suggested that for slow and heavy collision systems ($Z1/Z2 > 0.01$ and $v_2/v_1 < 0.01$), where perturbation of the projectile is very strong, the vacancies produced by direct ionisation could be rearranged among the subshells (Intra-Shell effect) before any rearrangement by Coster Kronig transitions. By treating the ionisation and the Intra-Shell effect (IS) as two successive steps of the same collision process, they initially introduced a classical two step model to account for the IS effect. Later on, full quantum mechanical treatment of this model were given by many other authors [20–23].

To demonstrate the efficacy of the Intra-Shell Coupling, all heavy ion induced data including ours, have been analysed by us [24] and Figure 4 shows our analysed results only for the $L2$ subshell ionisation.

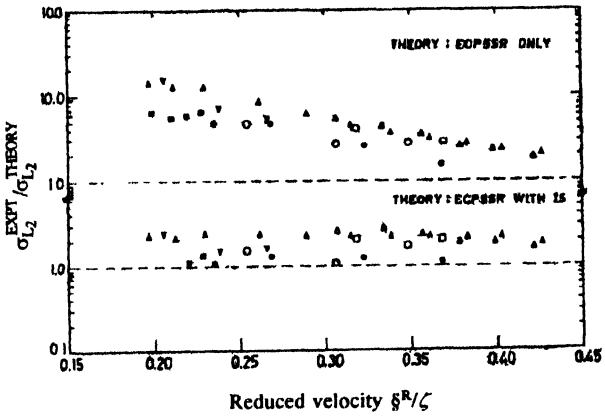

Figure 4. Ratio of the experimental and theoretical $L2$ subshell ionisation cross section for different projectile target combinations as a function of reduced velocity. Upper : calculations according to the ECPSSR theory; lower : the intra-shell effect has been combined with the ECPSSR.

Here all the data have been compared with the ECPSSR prediction with and without the inclusion of IS effect. The dimensionless quantity which has been shown along the x-axis is proportional to the velocity of the projectile. As can be seen from figure, inclusion of the IS effect inllie ECPSSR theory drastically improves its agreement with the measurements for $L2$ subshell ionisation cross sections. For the $L3$ subshell, the inclusion of the IS makes practically no difference. For the $L1$ subshell, however, it appears that the ECPSSR theory without IS effect gives better agreement with the data at $\xi^R/\zeta > 0.26$. Our conclusions are :

(1) The standard ECPSSR theory [15] without an account for IS coupling is confirmed to be quantitatively inadequate for the $L2$ subshell ionisation at low velocities; for the analysed heavy ion data this theory fails for $\xi^R/\zeta < 0.35$.

(2) The inclusion in the ECPSSR theory of the intra-shell effect substantially improves agreement between theory and experiment for the $L2$ subshell.

(3) The inclusion of the IS effect makes no essential difference in the analysis of of the $L1$ and $L2$ subshell data.

b. Alignment study :

Mehlhorn [25] had first pointed out that when a beam of charged particles ionises atoms, ions with vacancies in the subshell with angular momentum $J > \frac{1}{2}$ could be aligned with respect to the beam direction. The beam direction acts as the quantisation axis and the nonstatistical population distribution of the various magnetic substrates give rise to alignment which is reflected in non-isotropic emission of characteristic X-rays or Auger electrons from the target. The main reason to study the alignment is that it gives information about the population of the magnetic substrates of a particular subshell which is not possible to get from the total ionisation cross section measurement.

Let us take the case of the $L3$ ($2p_{3/2}$) subshell. It has a J value equal to 3/2 and so the possible m states are -3/2, -1/2, 1/2 and 3/2. Ignoring the -ve sign, the possible $|m|$ states are 3/2 and 1/2. Using the density matrix formalism [26], the degree of alignment A_2 can be expressed as

$$A_2 = \frac{\sigma_{3/2} - \sigma_{1/2}}{\sigma_{3/2} + \sigma_{1/2}} \tag{4}$$

Assuming that the nature of the characteristic X-rays are of dipole type, the angular distribution of the X-rays emitted from $J = 3/2$ state can be written as [27,28]

$$I(\theta) = \frac{I_0}{4\pi}[1 + \beta P_2(\cos\theta)] \tag{5}$$

where $\beta = \alpha\kappa A_2$

I_0 = Total emission rate of the specific X-rays

$I(\theta)$ = Rate of emitted X-rays at a particular angle θ

β = Measured anisotropy of the line

α = Angular momentum coupling constant between the initial and final states

κ = Correction factor due to the vacancies that are transferred from $L1$ and $L2$ subshell to $L3$ subshell through Coster-Kronig transition and is given by [29]

$$\kappa^{-1} = 1 + f_{23}\frac{\sigma_{L2}}{\sigma_{L3}} + (f_{13} + f_{12}f_{23})\frac{\sigma_{L1}}{\sigma_{L3}} \tag{6}$$

From equation (5), one can see that if $I(\theta)$ is plotted against $P_2(\cos\theta)$, the vaue of β could be experimentally determined. From the $L3$ subshell, the X-ray lines emitted are L_l, $L_{\alpha 1}$, $L_{\alpha 2}$ and $L_{\beta 1,3,5}$. The L_l line comprises of the singlet transition $3s_{1/2} \rightarrow 2p_{3/2}$. The other lines are doublet/multiplets and are inseparable when measured with a Si(Li) detector. So to have an idea of the $L3$ alignment, it is advisable to measure the angular distribution of the L_l line.

Before measuring the angular distribution of the L_l line, the angular anisotropy (if any) of our angular distribution table was measured using the $L_{\gamma 1}$ line of Au normalised to the number of scattered carbon ions and found to be about 3%.

The angular distribution of the L_l line was then measured in the range $60° \leq \theta \leq 150°$ and the normalised intensity (with respect to the $L_{\gamma 1}$ line) for one of such measurements (8.59 MeV carbon ions on Au) is shown in Figure 5.

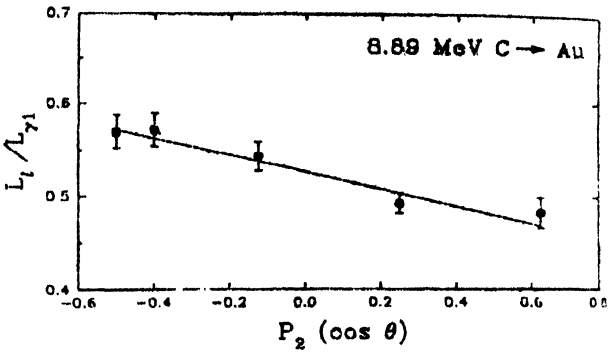

Figure 5. Angular distribution of the ratio $I_l/I_{\gamma 1}$ for 8.89 MeV C^{3+} ions on Au as a function of $P_2(\cos\theta)$. The straight line is the least square fit to the present data.

From such figures, the value of β parameters were obtained for all the energy points. The final results of the alignment parameter A_2(%) in the carbon impact on Au and Bi is shown in Figure 6 [30], where the scaled projectile velocity (velocity of the projectile/velocity of the target $L3$ electron) has been shown along the x-axis.

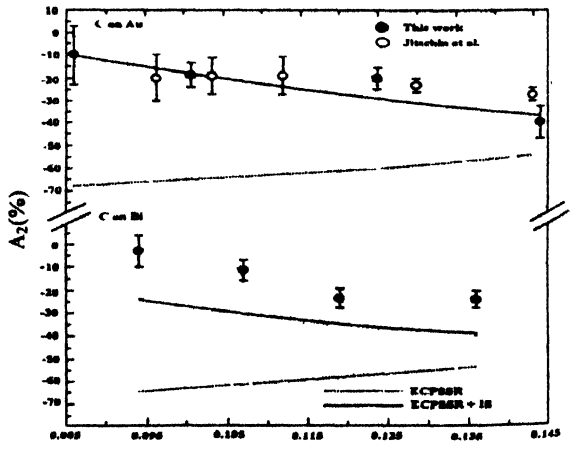

Figure 6. The measured values of the alignment parameter A_2 (%) in carbon impact on Au and Bi plotted as a function of projectile scaled velocity $V = v_l/v_{L3}$. • : this work; [30] : Jitschin *et al* [29]; ——ECPSSR, —ECPRRS + IS.

From Figure 6, it is clear that :

(1) The ECPSSR theory grossly underpredicts the data and the mismatch increases with decreasing projectile velocity.

(2) Inclusion of the IS factor substantially reduces the mismatch and for Au the agreement is seen to be quite good.

We had seen before that the inclusion of the IS effect into the ECPSSR did not change the $L3$ subshell cross section values [24]. This information coupled with the information from Figure 6 lead us to the important observation that it is the partition of the total $L3$ ($2p_{3/2}$) strength into the two magnetic substates $|mj| = 3/2$ and 1/2 that changes when the IS effect is included in the ECPSSR.

3.2. M Shell measurement

Next we turn to M shell measurements. Measurement of M X-rays is not as easy as that for K and L X-rays. The M shell has five subshells; so there are five fluorescence yields, ten Coster Kronig transitions and a number of radiative widths. The efficiency of a common Si(Li) detector at the energies of M X-rays is very low and the lines in the M group are not well resolved with such a detector. So the determination of subshell ionisation cross sections of different subshells or alignment parameter of a particular state is rather difficult. Our intererst on M shell measurements were two fold :

(i) to measure the anisotropy parameter (β) of the different M lines as seen by the Si(L) detector,

(ii) to measure the X-ray production cross sections of the different M lines and hence to obtain the total M X-ray ionisation cross section using the average fluorescence yields.

a. Anisotropy measurement :

When X-rays are emitted isotropically, one can use the relation

$$I_0 = I(\theta)\frac{4\pi}{\varepsilon d\Omega} \tag{7}$$

where I_0 is the total yield of X-rays, $I(\theta)$ is the X-ray yield measured at an angle θ, ε is the efficiency of the detector and $d\Omega$ is the solid angle subtended by the X-ray detector.

However, when X-rays are anisotropic, eqn. (7) is to be replaced by

$$I_0 = \frac{I(\theta)4\pi}{\varepsilon d\Omega[1+\beta P_2(\cos\theta)]} \tag{8}$$

where β is the anisotropy parameter of the particular X-ray line and $P_2(\cos\theta)$ is the second order Legendre polynomial.

In most of the X-ray production cross section measurements, the detector is placed at an angle of 90° to the beam and hence the numerical value of β (or at least the alignment parameter A_2) is required to obtain the value of I_0 in order to get the X-ray production/ionisation cross section.

From our discussion in 4.1b, it is clear that the K shell ($1s_{1/2}$, $J = 1/2$) X-rays are isotropic. For L shell, only the $L3$ ($2p_{3/2}$, $J = 3/2$) subshell would lead to the anisotropic emission of X-rays. The anisotropic emission of the different L lines have been thoroughly investigated by [29,30].

But for M X-rays, to the best of our knowledge, no measurements on β parameter have been done so far [31]. So with a Si(Li) detector, we measured the β parameter of different M lines of Au induced by carbon ions in the energy range 3–9 MeV. A typical spectrum of M X-rays fitted with the ACTIV program [32] is shown in Figure 7.

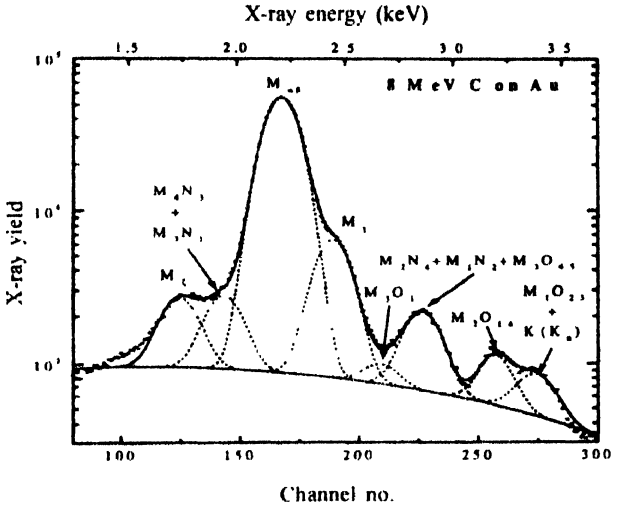

Figure 7. M X-ray spectrum of Au induced by 8 MeV C^{+2} ions and a typical fit of the spectrum with eight Gaussians using the program ACTIV [32].

Following the same procedure as has been done for L shell aniostropy, the anisotropy parameters (β) for various M X-ray lines were measured and are shown in Table 2 [33]. It is observed that M X-ray lines show large anisotropy, the measured parameter β, varying from 0.18 to 0.38. The uncertainty associated with the M lines is mainly due to the background fitting error.

b. Cross section measurement :

Using relation (3), the X-ray production cross section of different M lines, such as M_ζ, $M_{\alpha+\beta}$, M_γ *etc.* of gold and lead have been measured after bombarding with 4–12 MeV carbon ions [34]. Measured production cross sections of all these lines were then added together and using the average M shell fluorescence yield ($\bar{\omega}_m$), the total M shell ionisation

Table 2. Anisotropy parameter (β) for the various M X-ray lines of gold induced by carbon ions of different energies.

Energy	Anisotropy parameter (β) for the various M lines						
(MeV)	M_ζ	M_4–N_3 *etc*	$M_{\alpha\beta}$	M_γ	M_3–O_1	M_2–N_4 *etc.*	M_2–$O_{1,4}$
3.0	0.36 ± 0 21	0.27 ± 0.21	0.23 ± 0.05	0.17 ± 0.13	−0.14 ± 0.11	0.13 ± 0.03	0.10 ± 0 03
5.0	0.34 ± 0.33	0.25 ± 0.22	0.23 ± 0.05	0.17 ± 0.13	−012 ± 0.10	0.11 ± 0.03	0.17 ± 0.03
7.0	0.34 ± 0.32	0.21 ± 0.20	0.24 ± 0 05	0.17 ± 0.13	−0.14 ± 0.12	0:12 ± 0.03	0.14 ± 0 03
9.0	0.38 ± 0.33	0.20 ± 0.20	0.19 ± 0.05	0.14 ± 0.13	−0.17 ± 0.12	0.10 ± 0.03	0.17 ± 0.03

cross sections were obtained. Figure 8 shows our experimental results along with the data of others. ECPSSR and PWBA predictions are also shown. For both gold and lead, PWBA predictions are in fair agreement with the measured value; while ECPSSR predictions are a factor of 4 lower at the lowest energies. This is in sharp contrast to what has generally been observed for K and L cross section measurements where ECPSSR exhibit much better agreement with the data than the PWBA.

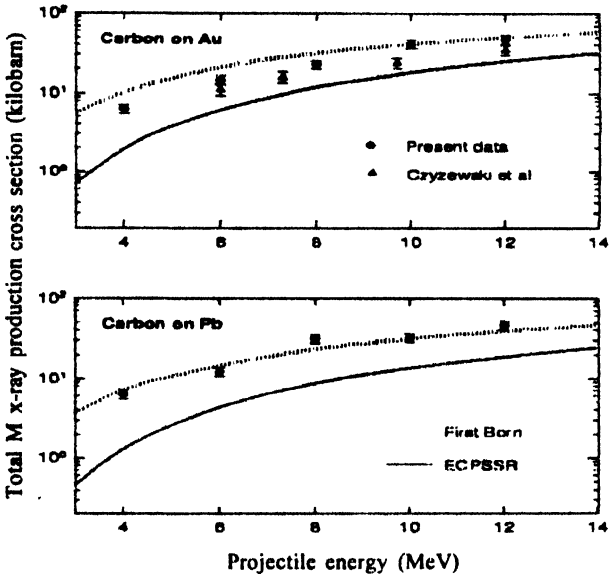

Figure 8. Total M X-ray production cross sections of Au and Pb induced by 4–12 MeV carbon ions. ------First Born; —ECPSSR; • Present data; ▲ data of Czyzewski *et al* [41].

3.3. K Shell measurement

a. Anisotropy measurement :

It has long been known that simultaneous multiple ionisation is a distinct possibility for ion-induced inner shell ionisation. The clear signature of multiple ionisation would be the presence of satellite lines in the X-ray spectrum taken with a high resolution crystal spectrometer. In spectra taken with a Si(Li) detector, the indication of the presence of multiple ionisation would be shift of centroids of the X-ray peaks on the higher energy side. It has been known since 1975 from curved crystal spectrometer data [35,36] that satellite lines emitted from single K multiple L (or M) vacancy states are strongly polarised. Accordingly, it is expected that X-rays emitted from such vacancy states would show strong anisotropy in their angular distribution. In the K X-ray spectrum taken with a Si(Li) detector, the satellite lines would not be separated from the diagram line and so the contribution of the anisotropic satellite lines should be reflected in the angular distribution of K_α or K_β line.

Following the same procedure as has been adopted for L X-ray anisotropy measurement, the anisotropy parameter for the K X-ray from Ge and Ag were measured for protons (0.83 and 0.93 MeV) and carbon (9.89 and 11.13 MeV) ions Table 3 shows the anisotropy parameter thus obtained for the K lines of Ge. We notice that–

(i) for the collision system studied here, protons show minimal deviation from isotropy and compared to protons, the anisotropy induced by carbon ions is larger. As our angular distribution table has an anisotropy of about 3%, so we are in no position to discuss about the minimal anisotropy that we have observed in the case of protons.

(ii) The K_β X-ray line induced by carbon ions is more anisotropic than the corresponding K_α line.

(iii) In the small range covered here, the K_β X-rays in carbon impact show about 4–8% deviation from isotropy.

Table 3. Anisotropy parameter (β) of the $K_{\alpha,\beta}$ X-rays of Ge induced by protons and carbon ions.

Energy (MeV)	Projectile	Anisotropy parameter (β) for K_α	Anisotropy parameter (β) for K_β
0.83	Proton	0.025 ± 0.002	0.020 ± 0.002
9.89	Carbon	0.041 ± 0.004	0.065 ± 0.014
0.93	Proton	0.026 ± 0.001	0.024 ± 0.008
11.13	Carbon	0.037 ± 0.003	0.080 ± 0.014

b. Cross section measurement :

We also measured the K X-ray production cross section of Ge and Ag induced by 3.7–11 MeV carbon ions [37]. Here the cross section measurements were done relative to the measurements with protons. Figure 9 shows our experimental values only for Ge. Both the ECPSSR and the Molecular Orbital (MO) theory of Montenegro and Sigaud [38] are also

displayed in Figure 9. Our measurements show excellent agreement with ECPSSR for Ag (not shown) but for Ge and low energies, we need MO theory. It seems to indicate that perhaps the boundary of validity of the MO approach should be somewhat extended at the expense of the ECPSSR formulation when viewed as shown in Figure 1 of Lapicki and Litchen [39].

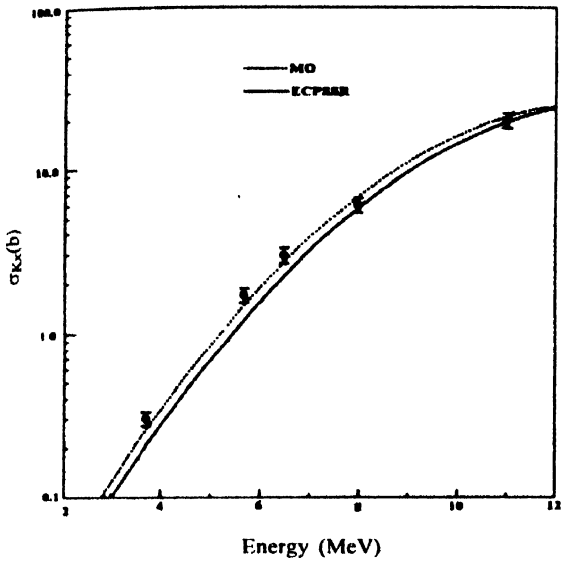

Figure 9. *K* X-ray production cross section of Ge induced by carbon ions

4. Conclusion

More investigations could be done on *L* subshell ionisation with heavy ions. An interesting study would be to measure these cross sections and also the alignment as a function the impact parameter of the projectile.

As there are only a few data on *M* shell cross sections induced by heavy ions, in order to investigate the effect of CIS on *M* shell data, it would be necessary to measure individual subshell ionisation cross sections for the *M* shell. This would make it mandatory to use a crystal spectrometer to detect the X-ray.

It would also be interesting to carry out *K* shell ionization measurements in the low energy range with heavy ions especially on low *Z* elements to investigate the differences that emerge when compared with the ECPSSR theory, and to probe the territory where the MO approach becomes preferable to the ECPSSR theory.

We have already mentioned that Simultaneous Multiple Ionisation (SMI) occurs in the outer shells while producing vacancies in the inner shells. This SMI effect is supposed to change the atomic parameters like fluorescence yields (ω_i), Coster Kroning transition rates (f_{ij}) and radiative widths (Γ_i). Although there are some scaling laws [40] to incorporate the effect of SMI in the *K* shell fluorescence yields, to the best of our knowledge, no effort has been made experimentally to investigate the extend of the changes of these atomic parameters in the case of heavy ion induced ionisation. It would therefore be very interesting to experimentally determine the values of these parameters *in situ*.

Acknowledgment

Author is thankful to Dr. D Mitra for his help in making this manuscript camera ready.

References

[1] W C Röentgen *Sitzengsberichte derWürzburger Physik Medig Gesellshaft* (1995); *Ann. Phys.* **64** 1 (1898)

[2] J Chadwick *Phil. Mag.* **24** 594 (1912)

[3] H Franz and W Bothe *J Franklin Inst.* **52** 466 (1928)

[4] C Grethsen and W Reusse *Phys. Z.* **34** 478 (1933)

[5] O Peter *Ann Phys. Leipzig* **27** 299 (1936)

[6] M S Livingston, F Genevese and E J Konopinski *Phys, Rev* **51** 835 (1937)

[7] T B Johansson, R Akselsson and S A E Johensson *Nucl Instr. & Methods* **84** 141 (1970)

[8] E Merzbacher and H W Lewis *Handbuch der Physik* ed. S Fliigge (Berlin : Springer-Verlag) 166 (1958)

[9] G S Khandelwal, B H Choi and E Merzbacher *At. Data* **1** 103 (1969)

[10] R Rich, G Basbas and F D McDaniel *At Data Nucl. Data Tables* **20** 503 (1977)

[11] O Benka and A Kropf *At. Data Nucl Data Tables* **22** 219 (1978)

[12] J D Garcia *Phys Rev.* **A1** 280 (1970)

[13] J Bang and J M Hansteen *Kgl Dan. Vidensk. Selsk. Mat. Fys. Medd.* **31** 13 (1959)

[14] D Trautmann and F Rosel *Nucl. Instr. & Methods* **169** 259 (1980)

[15] W Brandt and G Lapicki *Phys. Rev.* **A23** 1717 (1981)

[16] H Paul and J Sacher *At. Data Nucl. Data Tables* **42** 105 (1989)

[17] S Datz, J L Duggan, L C Feldman, E Laegsgaard and J U Andersen *Phys. Rev.* **A9** 192 (1974)

[18] D Bhattacharya, M Sarkar, M B Chatterjee, P Sen, G Kuri, D P Mahapatra and L G Lapicki *Phys. Rev.* **A49** 4616 (1994)

[19] L Sarkadi and Mukoyama *J. Phys.* **B14** L255 (1981)

[20] L Sarkadi and T Mukoyama *Phys. Rev.* **A37** 4540 (1988); *J. Phys.* **B23** 3849 (1990); *Nucl. Instr. & Methods* **B61** 167 (1991)

[21] R Singhal, N B Mahil and T J Gray *J. Phys.* **B25** 2055 (1992)

[22] P A Amundsen and D R Jakubassa-Amundsen *J. Phys.* **B21** L99 (1988)

[23] I C Legrand, V Zoran, L Dörner, R Schmidt-Bocking, A Berinde, D Fluerasu and C Ciortea *J. Phys.* **B25** 189 (1992)

[24] M Sarkar, D Bhattacharya, M B Bhattacharya, P Sen, G Kuri, D P Mahapatra and G Lapicki *Nucl. Instr. & Methods* **103** 23 (1995)

[25] W Mehlhorn *Phys. Lett.* **A26** 166 (1968)

[26] K Blum *Density Matrix Theory and Application* (New York : Plenum) (1981)

[27] E G Berezkho and N M Kabachnik *J. Phys.* **B10** 2467 (1977)

[28] V V Sizov and N M Kabachnik *J. Phys.* **B16** 1565 (1983)

[29] W Jitschin, R Rippler, R Shanker, R Kleipoppen, R Schuch and R O Lutz *J. Phys.* **B16** 1417 (1981)

[30] D Mitra, M Sarkar , D Bhattacharya, M B Chatterjee, P Sen, G Kuri, D P Mahapatra and G Lapicki *Phys. Rev.* **A53** 2309 (1996)

[31] Y C Yu, R L Sun, J L Duggan, F D McDaniel, J Y Yin and G Lapicki *Phys. Rev.* **A52** 3836 (1995)

[32] V B Zlokazov *Comp. Phys. Comm.* **28** 27 (1982)

[33] D Mitra, M Sarkar, D Bhattacharya, P Sen and G Kuri *Nucl Instr. & Methods* **B145** 283 (1998)

[34] D Mitra, A C Mandal, M Sarkar, D Bhattacharya, P Sen and G Lapicki (to be published)

[35] K A Jamison and P Richard *Phys. Rev. Lett.* **38** 484 (1977)

[36] K A Jamison, P Richard, F Ropkins and D L Metthews *Phys Rev.* **A17** 1642 (1978)

[37] D Mitra, M Sarkar, D Bhattacharya, P Sen, G Kuri and G Lapick.. *Nucl Instr. & Methods* **B124** 453 (1997)

[38] E C Montengro and G M Sigaud *J Phys.* **B18** 299 (1985)

[39] G Lapicki and W Lichten *Phys. Rev.* **A31** 1354 (1985)

[40] D Burch, L Wilets and W E Meyerhof *Phys. Rev* **A9** 1067 (1974)

[41] T Czyzewski, L Glowacka, M Jaskola, J braziewicz, M Pajek J Samaniak, M hailer, R Karschnick, W Kretschmer, A P Kobzev and D Trautmann *Nucl. Istr. & Methods* **B109/110** 52 (1996)